

DETERMINATION OF STELLAR ATMOSPHERIC PARAMETERS FOR A SAMPLE OF THE POST-AGB STARS

R. E. Molina,¹

Received ; accepted

RESUMEN

Reportamos por primera vez los parámetros atmosféricos estelares para un conjunto de estrellas clasificadas como post-AGB por Suárez et al. (2006). Los espectros estelares empleados para el estudio fueron tomados en la región óptica, con baja resolución y poseen diferentes rangos espectrales. Seleccionamos una muestra de 70 objetos con tipos espectrales que abarcan un rango entre A–K y clases de luminosidades I y Ie. La mayoría de las estrellas han sido poco estudiadas y se encuentran ubicadas hacia la región del polo sur galáctico. Se emplean un conjunto de calibraciones empíricas que utilizan los pseudo anchos equivalentes como característica espectral para estimar la temperatura efectiva, la gravedad superficial y la metalicidad. Los criterios tomados para la selección de las líneas de absorción son similares a los empleados por el sistema MK.

ABSTRACT

We report for the first time the stellar atmospheric parameters for a set of post-AGB stars classified by Suárez et al. (2006). The stellar spectra were taken from optical region, with low-resolution and have different spectral ranges. We select a sample of 70 objects with A–K spectral types and luminosities I and Ie. The large majority of these objects have been scarcely studied and are located toward the galactic south pole region. We employ a set of empirical relationships that use pseudo-equivalent widths like spectral feature to estimate effective temperature, surface gravity and metallicity. The criteria chosen for selection of absorption are similar to employed by MK classification system.

Key Words: Stars: equivalent widths — Stars: stellar atmospheric parameters — Stars: post-AGB

1. INTRODUCTION

When performing a detailed analysis of the chemical abundances, it is essential to estimated as accurately as possible the relevant physical parameters that will lead the choice of the proper atmospheric models, i.e. effective temperature, surface gravity, and micro-turbulence velocity. This can be achieved from a variety of photometric (e.g. Arellano Ferro, Mendoza & Eugenio 1993; Schuster et al. 1996; Alonso et al. 1999; Mauro et al. 2013) and spectroscopic methods (e.g. Gray et al. 2001; Giridhar & Goswami 2002; Molina & Stock 2004; Soubiran et al. 2010; Wu et al. 2011, Chen et al. 2015; Teixeira et al. 2016).

Stellar atmosphere is characterized mainly by T_{eff} , $\log g$, ξ_t and $[\text{Fe}/\text{H}]$, and the knowledge of these parameters is crucial in many research areas related to the stellar and galaxy physics.

The traditional spectroscopic method to initially derive the effective temperature and gravity is via the ionization equilibrium of a well represented specie, such as that of Fe I and Fe II or Ti I and Ti II and a set of stellar models such as ODFNEW-ATLAS9 (Castelli & Kurucz 2003) and MARCS (Gustafsson et al. 2008).

Empirical calibrations to estimate the stellar parameters employ, besides equivalent widths, other quantifiable spectroscopic features such as the central residual intensities and pseudocontinuum peaks (Rose 1984), relative depth ratios (Kovtyukh et al. 2003) and photometric bandheads (Árnadóttir et al.

¹Laboratorio de Investigación en Física Aplicada y Computacional, Universidad Nacional Experimental del Táchira, CP 5001, Venezuela.

TABLE 1
EQUIVALENT WIDTHS FOR WARM STARS.

IRAS number	SpT	CaIIK 3933 (Å)	Fe,TiII 4172-9 (Å)	FeI blend 4271 (Å)	FeI 4383 (Å)	OI 7771-5 (Å)	ref.
02143 + 5852	F7Ie	1.01	0.18	0.32	0.05	...	01
02528 - 4350		1.26	0.19	0.13	
04296 + 3429	F7I	01
05341 + 0852	F5I	...	1.94	0.23	0.29	1.52	01
06530 - 0213	F0Iab	...	2.40	0.80	3.23	...	02
07134 + 1005	F7Ie	...	1.25	0.27	0.31	...	01
07253 - 2001	F2I	0.27	...	01
07430 + 1115	G5Ia	0.99	...	04
08005 - 2356	F5Ie	4.68	1.42	...	0.73	1.27	01
08143 - 4406	F8I	8.39	2.09	0.48	0.99	...	05
08187 - 1905	F6Ib/II	0.24	...	03
08213 - 3857	F2Ie	...	0.74	0.19	0.22	...	01
08281 - 4850	F0I	1.22	0.94	2.74	1.65	1.90	01
10215 - 5916	A7Ie	11.32	4.22	2.37	3.12	1.77	01
10256 - 5628	F5I	12.72	1.38	1.75	0.42	2.17	01
11201 - 6545	A3Ie	0.48	...	01
11387 - 6113	A3Ie	...	0.74	0.30	0.44	...	01
12067 - 4505	F6I	0.05	...	06
14325 - 6428	A8I	6.18	1.10	0.24	0.96	...	07
14429 - 4539	A1I	0.91	1.05	0.23	0.47	1.85	02
14482 - 5725	A2I	1.13	...	01
14488 - 5405	A0I	0.02	...	01
15039 - 4806	A5Iab	0.75	0.50	0.12	0.21	1.64	08
15310 - 6149	A7I	0.09	...	01
15482 - 5741	F7I	...	1.88	0.33	0.22	...	01
16283 - 4424	A2Ie	4.50	0.25	3.00	1.58	2.38	01
17106 - 3046	F5I	9.62	2.68	1.25	0.58	2.10	01
17208 - 3859	A2I	...	0.57	0.23	0.82	...	01
17245 - 3951	F6I	9.13	2.00	1.49	2.13	2.02	01
17287 - 3443		0.96	0.10	0.15	0.14	0.74	
17310 - 3432	A2I	...	0.36	0.22	...	1.30	01
17376 - 2040	F6I	01
17436 + 5003	F3Ib	6.76	1.88	1.14	1.07	...	09
17441 - 2411	F4I	7.38	1.16	0.99	0.52	2.06	01
17488 - 1741	F7I	01
17576 - 2653	A7I	5.13	0.85	0.02	0.58	2.12	01
17579 - 3121	F4I	...	2.42	0.24	0.98	...	01
18025 - 3906	G1I	13.14	2.18	0.22	1.30	...	01
18044 - 1303	F7I	01
19114 + 0002	G5Ia	9.86	3.90	1.82	1.59	...	10
19207 + 2023	F6I	...	3.44	...	3.74	...	01
19386 + 0155	F5I	8.31	1.20	1.70	0.97	1.66	11
19422 + 1438	F5I	01
19500 - 1709	F0Ie	1.67	0.95	0.44	0.74	1.94	01
19589 + 4020	F5I	01
20160 + 2734	F3Ie	4.52	1.95	1.28	1.33	...	01
20259 + 4206	F3I	01
20572 + 4919	F3Ie	4.41	0.92	0.73	0.63	...	01
21289 + 5815	A2Ie	0.68	1.12	1.94	0.76	...	01
22223 + 4327	F7I	8.93	2.41	1.05	1.02	...	01

TABLE 2
EQUIVALENT WIDTHS FOR COLD STARS.

IRAS number	SpT	FeI 4063 (Å)	SrII 4077 (Å)	CaI 4226 (Å)	G-band 4302 (Å)	FeI 4383 (Å)	OI 7771-5 (Å)	ref.
01259 + 6823	G1ab:	0.76	2.95	1.34	3.60	0.48	...	12
05113 + 1347	G5I	1.76	1.37	...	12
05381 + 1012	G2I	0.37	0.76	0.40	2.87	0.51	...	04
07331 + 0021	G5Iab	...	1.70	0.77	3.60	0.88	...	10,13
07582 - 4059	G5I	...	1.60	0.98	5.69	2.86	...	01
10215 - 5916		1.53	3.03	3.12	1.77	01
13203 - 5917	G2I	5.02	6.31	4.94	...	01
13313 - 5838	K5I	2.86	...	2.31	4.07	1.94	0.06	01
15210 - 6554	K2I	...	3.28	1.54	7.65	1.87	0.98	01
16494 - 3930	G2I	1.13	2.54	0.82	1.38	01
17300 - 3509	G2I	...	1.18	1.08	5.21	1.30	...	01
17317 - 2743	G4I	2.66	...	1.59	2.06	1.68	2.07	14
17332 - 2215	K2I	...	1.20	1.72	5.35	3.93	0.46	01
17370 - 3357	G3I	0.27	0.27	0.67	2.53	2.39	1.88	01
17388 - 2203	G0I	1.34	1.34	0.30	3.52	0.99	1.78	01
18075 - 0924	G2I	1.21	...	0.91	1.66	1.86	...	01
18096 - 3230	G3I	1.69	0.16	1.57	6.02	1.68	...	01
18582 + 0001	K2I	...	1.51	...	4.62	2.64	...	01
19356 + 0754	K2I	...	2.90	1.62	6.51	2.90	...	01
19477 + 2401	G0I	14

(01) Suárez et al. (2006); (02) Hu et al. (1993); (03) Hrivnak et al.(1989); (04) Fujii et al. (2001); (05) Hrivnak & Biegging (2005); (06) Maas et al. (2002); (07) Reyniers et al. (2007); (08) Stephenson & Sanduleak (1971); (09) Min et al. (2013); (10) Omont et al. (1993); (11) Hrivnak, Lu & Nault (2015); (12) Kelly & Hrivnak (2005); (13) Klochkova (1997); (14) Sánchez-Contreras et al. (2008)

TABLE 3
ATMOSPHERIC PARAMETERS USED AS CALIBRATORS TAKEN FROM LITERATURE.

IRAS number	SpT	$T_{\text{eff}}^{\text{ref}} \pm \Delta T_{\text{eff}}^{\text{ref}}$ (K)	$\log g^{\text{ref}} \pm \Delta \log g^{\text{ref}}$	$[\text{Fe}/\text{H}]^{\text{ref}} \pm \Delta [\text{Fe}/\text{H}]^{\text{ref}}$ (dex)	ref.
Warm stars ($6000 \leq T_{\text{eff}} \leq 8000 \text{ K}$)					
15039 – 4806	A0I	8000±200	1.25±0.25	-0.85±0.10	07
14325 – 6428	A8I	8000±125	1.00±0.25	-0.56±0.16	03
19500 – 1709	F0Ie	8000±125	1.00±0.25	-0.59±0.10	03
08281 – 4850	F0I	7875±125	1.25±0.25	-0.26±0.11	03
20572 + 4919	F3Ie	7500±200	2.00±0.50	-0.01±0.10	13
15482 – 5741	F7I	7400±150	1.40±0.20	-0.47±0.16	08
06530 – 0213	F0Iab:	7375±125	1.25±0.25	-0.32±0.11	03
08005 – 2356	F5Ie	7300±250	06
07134 + 1005	F7Ie	7250±200	0.50±0.30	-1.00±0.20	04
08143 – 4406	F8I	7150±100	1.35±0.15	-0.39±0.12	15
17436 + 5003	F3Ib	7065±125	0.91±0.15	-0.09±0.10	09
04296 + 3429	F7I	7000±250	1.00±0.50	-0.69±0.20	02
19386 + 0155	F5I	6800±100	1.40±0.20	-1.10±0.15	12
19114 + 0002	G5Ia	6750±200	0.50±0.25	-0.45±0.20	11
05341 + 0852	F5I	6500±200	1.00±0.50	-0.72±0.12	04
22223 + 4327	F7I	6500±125	1.00±0.25	-0.30±0.11	03
08187 – 1905	F6Ib	6250±200	0.50±0.20	-0.59±0.15	01
18025 – 3906	G1I	6250±100	0.25±0.25	-0.45±0.16	10
20259 + 4206	F3I	6100±200	2.20±0.25	-0.10±0.15	10
12067 – 4508	F6I	6000±250	1.50±0.50	-2.00±0.12	16
07430 + 1115	G5Ia	6000±125	1.00±0.25	-0.33±0.15	03
Cool stars ($4500 \leq T_{\text{eff}} \leq 5500 \text{ K}$)					
05113 + 1347	G5I	5500±125	0.50±0.25	-0.54±0.17	03
05381 + 1012	G2I	5200±100	1.00±0.50	-0.80±0.17	05
01259 + 6823	G1ab:	5000±200	1.50±0.25	-0.60±0.12	01
13313 – 5838	K5I	4540±150	2.20±0.30	-0.09±0.05	14
07331 + 0021	K3/K5I	4500±200	1.00±0.25	-0.16±0.16	01

(01) Rao, Giridhar & Lambert (2012); (02) Decin et al. (1998); (03) De Smedt et al.(2016); (04) Reyniers & van Winckel (2000); (05) Pereira & Roig (2006); (06) Klochkova (2014); (07) van Winckel, Oudmaijer & Trams (1996); (08) Pereira, Gallino & Bisterzo (2012); (09) Luck (2014); (10) Molina et al., in preparation; (11) Kipper (2008); (12) Pereira, Lorentz- Martins & Machado (2004); (13) Klochkova et al. (2008); (14) Drake et al. (2012); (15) Reyniers et al. (2004); (16) Maas et al. (2002).

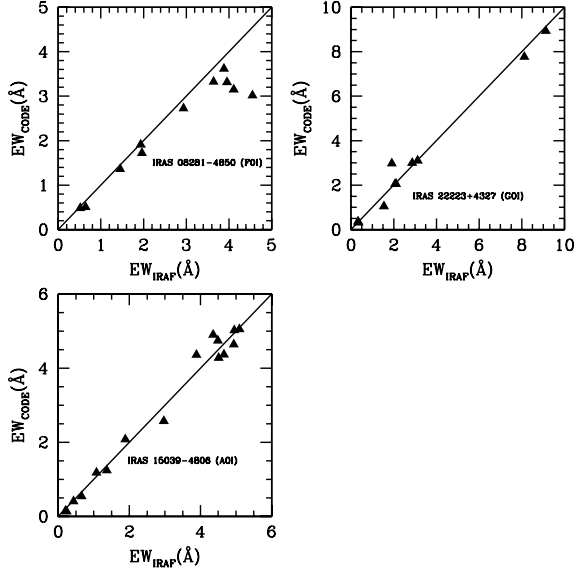


Fig. 2. Correlation between the equivalent widths measured with the automatic code with those taken from IRAF code. Three objects IRAS 01919 + 0373, IRAS 08281 - 4850, IRAS 22223 + 4327 with spectral types A0, F0 and G0 has been used to compare their results.

at $\lambda 4383\text{\AA}$) preventing the estimation of their fundamental parameters. In cold-PAGB stars, on the other hand, only one object does not have measures of the equivalent width.

2.1. Determination of equivalent widths

The quantification of equivalent widths was done in an automatic manner. In this sense we have developed a code that replaces the true continuum by a pseudo-continuum through the interpolation of a straight line that connect the peaks on both sides of an absorption line (see Figure 1).

The equivalent width is then defined as the effective area occupied between the two maximum interpolated $W_j = \sum_{j=1}^n \frac{(I_c - I_j)}{I_c} \Delta\lambda$, where $\Delta\lambda$ is a wavelength interval (or its dispersion). Table 1 and 2 shows the quantified measures of 9 equivalent widths of absorption lines selected in this study.

We can compare the measurements of equivalent widths from the automatic code and those done manually with the IRAF code. We use the quantifiable parameters of IRAS 01919 + 0373, IRAS 08281 - 4850, IRAS 22223 + 4327 with spectral types A0, F0 and G0 respectively. From Figure 2 we note that for weaker absorption lines (i.e. with low measures and intermediate equivalent widths) their values are in good agreement among themselves, while for stronger lines their values show slight systematic

differences between them, which increase slightly its error. The outliers obtained with this method are usually due to poorly measured of the equivalent widths caused by a poor maximum points determination.

2.2. MK criteria

Our atmospheric parameters were estimated from features used by the MK system.

In determining the effective temperature we have used the equivalent widths of the calcium line Ca IIK at $\lambda 3933\text{\AA}$ (warm stars) and the G-band at $\lambda 4302\text{\AA}$ (cool stars). The Ca IIK feature grows dramatically in strength of A-type toward to late types ($\sim F8$), for cooler spectral types their equivalent widths remain flat. Other features as Ca I at $\lambda 4226\text{\AA}$ and Mn I at $\lambda 4030\text{\AA}$ blend are not useful to estimating the temperature in warm stars.

In the G-type stars, the G-band characteristically dominates over other features. This feature increase in strength until about K2 and then decreases in intensity. Another feature as Mg I at $\lambda 5167-72\text{\AA}$ triplet shows some sensitivity to temperature for cold objects.

For the surface gravity we employ ionized lines like criteria for its determination ($\lambda 4172-79\text{\AA}$ and $\lambda 4395-4400\text{\AA}$ blends, Sr II at $\lambda 4077\text{\AA}$ and Mg II at $\lambda 4481\text{\AA}$). It is also possible to use the neutral oxygen (O I triplet $\lambda 7771-5\text{\AA}$) located in the near IR-region. In warm stars, however, only the $\lambda 4172-79\text{\AA}$ blend of Fe II and Ti II shows sensitivity to the gravity. While the Sr II at $\lambda 4077\text{\AA}$ and Ca I at $\lambda 4226\text{\AA}$ lines show sensitivity to gravity in cold stars.

In order to obtain the stellar metallicity we used only absorption lines of neutral iron, i.e. Fe I ($\lambda 4063\text{\AA}$), Fe I ($\lambda 4271\text{\AA}$) blend and Fe I ($\lambda 4383\text{\AA}$). We discard any ionized iron lines because of their expected dependence on $\log g$. In warm stars, we use as metallicity indicator the sum of iron lines Fe I ($\lambda 4271\text{\AA}$ blend + $\lambda 4383\text{\AA}$), while the Fe I ($\lambda 4063\text{\AA}$ and $\lambda 4383\text{\AA}$) were employed in cool stars.

The lines of Na ID at $\lambda 5889-95\text{\AA}$ and O I T at $\lambda 7771-5\text{\AA}$ are used as probable indicators for the determination of the stellar distance. The interstellar component of Na ID lines at $\lambda 5889-95\text{\AA}$ show sensitivity to luminosity in young stars, however, in evolved stars (as PAGB stars) both lines are affected by circumstellar material and therefore does not show dependence to luminosity. The O I T lines at $\lambda 7771-5\text{\AA}$, on the other hand, also show sensitivity to luminosity. In fact, Arellano Ferro et al.(2003) found accurate spectroscopic calibrations between visual absolute magnitudes and the O I T lines for

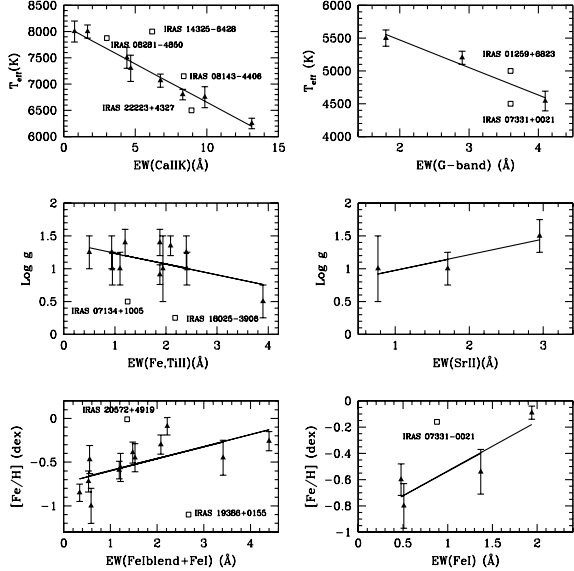


Fig. 3. Trend of dispersion σ_{EW} with the spectral type. We see that dispersion shows a tendency to increase with the increase of the spectral type in both warm and cold stars.

a sample of 27 calibrator stars with spectral types A to G.

Because of the spectral range limitation in the near infrared region, the lines of hydrogen Paschen series, the oxygen and calcium triplet lines are very rare in the total sample. The equivalent widths of all features are represented in Table 1 and 2, respectively.

2.3. Error in the equivalent widths

An accurate determination of systematic and random errors of the equivalent widths is not trivial, since these come to be a function of the magnitude, spectral type, the S/N ratio and the pseudo-continuum position. We also need common stars with the same spectral types and several measures of their stellar spectra. This sample has limitations of objects with the same spectral types and also with scarce measurements of equivalent widths, which is impossible to carry out a reliable statistics.

In this section we can estimate an approximation between the errors of the equivalent widths of the selected absorption lines and the spectral types. In this sense, the spectral types were replaced by numerical values in the following sequence: A0 = 30, F0 = 40, G0 = 50 and K0 = 60 respectively. The intermediate values are between two successive classes. In view of the difficulties presented by the observational data (mentioned in the above paragraph), we decided to correlate the equivalent widths determined through

the automatic code with those obtained from the IRAF code for both samples as shown in Figure 2.

A dispersion, σ_{EW} , is obtained for each spectral type (or an average σ_{EW} , if the spectral type is repeated), which varies from 0.02 to 0.47 in the warm stars and from 0.15 to 0.35 in the cold stars. In Figure 3 we observe that the dispersion shows a tendency to increase with the increase of the spectral type in both warm and cold stars. This dispersion results in an error in the effective temperature, ΔT_{eff} , such that using the equation 1 leads to a variation between 5 K to 68 K and from 63 K to 122 K using equations 2 and 3 respectively.

With these arguments we can infer that the new spectroscopic calibrations in effective temperature, gravity and metallicity are not affected by the dispersion in the equivalent widths.

2.4. Sample for calibration

Table 3 shows the PAGB stars that have been studied and reported in the literature. This table contains the number IRAS, spectral type, the stellar atmospheric parameters obtained from different sources and their respective references. Their stellar parameters were obtained by different authors using spectroscopic methods.

We can observe that there are a total of 21 stars considered as warm-PAGB stars and a very small number of only 5 objects for the cold-PAGB stars. In spite of having a small number of stars as calibrators is possible to obtain a rapid and accurate determination of fundamental parameters (effective temperature, the surface gravity and the metallicity) using only suitable spectral criteria, avoiding photometric indices which are often distorted by poor known interstellar and circumstellar reddening.

In the recent past, two papers that involve photometric calibrations (Strömgren and 2MASS photometry) and that allows to estimate the stellar parameters for a group of post-AGB and RV Tauri stars were done by Arellano Ferro et al. (2010) and Molina (2012).

2.5. Polynomial's fitting

The stellar atmospheric parameters can be determined by fitting a series of polynomials whose independent variables are equivalent widths. Our goal is to analyze the actual dependence of the stellar parameters with respect to one or two quantifiable features. The mathematical representation of the polynomial, in general, has the form

$$V = a_{00}x + a_{01}y + a_{02}xy,$$

TABLE 4
 ATMOSPHERIC PARAMETERS ESTIMATED FROM
 EQUIVALENT WIDTHS FOR WARM STARS.

IRAS number	$T_{\text{eff}}^{\text{phot}}$ ($\pm 220\text{K}$)	$T_{\text{eff}}^{\text{eq}1}$ ($\pm 91\text{K}$)	$\log g^{\text{phot}}$ (± 0.27)	$\log g^{\text{eq}4}$ (± 0.21)	$[\text{Fe}/\text{H}]^{\text{eq}7}$ (± 0.19)
02143 + 5852	...	7967	-0.68
02528 - 4350	...	7981	-0.71
07253 - 2001	...	7826	1.39	1.28	-0.81
08005 - 2356	1.32	1.17	-0.92
08213 - 3857	...	7872	...	1.28	-0.67
10215 - 5916	...	6461
10256 - 5628	...	6257	0.85	1.18	-0.42
11201 - 6545	...	7723	...	1.26	-0.86
11387 - 6113	6209	7707	0.75	1.28	-0.63
13245 - 5036 ¹	7077	...	0.77
14429 - 4539	...	7981	0.95	1.23	-0.63
14482 - 5725	...	7402	...	1.13	-1.01
14488 - 5405	7578	7950	0.86	1.28	-0.75
15310 - 6149	5787	7915	0.98	1.35	-0.77
16206 - 5956 ¹	7382	...	0.86
16283 - 4424	5699	7457	0.82	...	-0.09
17106 - 3046	...	6709	...	0.97	-0.47
17208 - 3859	5734	7856	0.96	1.31	-0.58
17245 - 3951	...	6781	0.91	1.08	-0.22
17287 - 3443	...	8024	-0.69
17310 - 3432	...	7869
17376 - 2040 ²
17441 - 2411	5404	7037	0.95	1.21	-0.52
17488 - 1741 ²	5860	...	0.73
17576 - 2653	7026	7365	...	1.26	-0.64
17579 - 3121	5845	7790	0.78	1.01	-0.56
18044 - 1303 ²
19207 + 2023	4785	6638	0.71	0.85	...
19422 + 1438 ²	6383	...	0.72
19589 + 4020 ²	5231	...	0.78
20160 + 2734	6168	7454	0.80	1.09	-0.36
21289 + 5815	...	8015	...	1.22	-0.35

¹ Emission lines.

² Not has measured EWs.

TABLE 5
ATMOSPHERIC PARAMETERS ESTIMATED FROM EQUIVALENT WIDTHS FOR COLD STARS.

IRAS number	$T_{\text{eff}}^{\text{phot}}$ ($\pm 220\text{K}$)	$T_{\text{eff}}^{\text{eq2}}$ ($\pm 207\text{K}$)	$T_{\text{eff}}^{\text{eq3}}$ ($\pm 175\text{K}$)	$\log g^{\text{phot}}$ (± 0.27)	$\log g^{\text{eq6}}$ (± 0.20)	$[\text{Fe}/\text{H}]^{\text{eq8}}$ (± 0.30)
07582 – 4059	5042	...	1.12	...
10215 – 5916	...	5027	4852
13203 – 5917	6355	1.23	...
15210 – 6554	4848	0.74	...	-0.21
16494 – 3930	6227	5232	4990	...	1.15	-0.61
17300 – 3509	5007	1.10	1.02	-0.43
17317 – 2743	...	5432	4831	...	1.14	-0.28
17332 – 2215	4786	...	1.03	...
17370 – 3357	4869	5236	5149	-0.78 ^a
17388 – 2203	5267	4823	1.06	-0.54
18075 – 0924	5517	5599	5066	...	1.23	-0.21
18096 – 3230	4838	0.75	...	-0.28
18582 + 0001	1.10	...
19356 + 0754	4820	...	1.44	...
19477 + 2401

where V is any of the three stellar parameters (T_{eff} , $\log g$ and $[\text{Fe}/\text{H}]$), a_{ij} are the coefficients to determine and x and y are the independent variables. When the number of independent variables is greater than one we used the method adopted by Stock & Stock (1999). This method developed a quantitative method to obtain stellar physical parameters such as absolute magnitude, intrinsic colour, and a metallicity index using the equivalent widths of absorption features in stellar spectra by means of polynomials and a consistent algorithm (Molina & Stock 2004).

In order to determine the best coefficients we employ an algorithm based on least squares. This algorithm performs an initial fitting and removes those values of residuals greater than 2σ . The error of each coefficient is obtained from

$$\sigma_{a_{ij}}^2 = \sigma^2 S(i, j),$$

where $S(i, j)$ the diagonal matrix and σ^2 is the mean square error.

3. STELLAR ATMOSPHERIC PARAMETERS

The main objective of this work is to build a set of spectroscopy calibrations to derive T_{eff} , $\log g$ and $[\text{Fe}/\text{H}]$ for PAGB stars. We employ the data contained in Tables 1, 2 and 3. In this section we will show the best fits when comparing the equivalent widths with the stellar atmospheric parameters taken from literature.

3.1. T_{eff} 's calibration

For the determination of effective temperature in warm-PAGB stars we use equivalent widths of

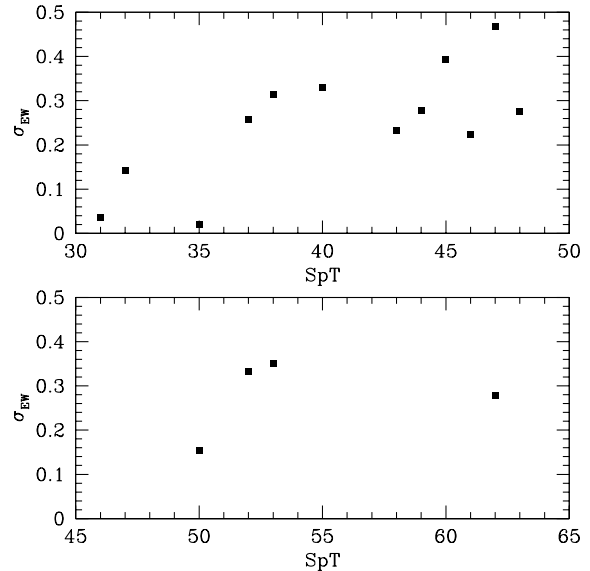


Fig. 4. Relation between the stellar atmospheric parameters as a function of equivalent widths for warm stars (left panel) and cold stars (right panel). Left panel. The empty squares represent those stars that left out of the best fit.

the Ca I K at $\lambda 3933 \text{ \AA}$. This line has been considered in the MK system as an indicator of temperature in warm stars (Gray & Corbally 2008). Particularly, for stars with temperature between ($6000 \leq T_{\text{eff}} \leq 8000 \text{ K}$), the equivalent widths show sensitivity to effective temperature. A code based on least squares that relates equivalent widths and the effective temperature taken from literature ($T_{\text{eff}}^{\text{ref}}$) leads to the following relationship

$$T_{\text{eff}} = (8114 \pm 65) - (146 \pm 24)(\text{Ca I K}), \quad (1)$$

where this calibration is valid for a range in the equivalent widths between $0.76 \leq T_{\text{eff}} \leq 13.15 \text{ \AA}$. The standard deviation derived from the equation (1) is $\pm 91 \text{ K}$. Four stars are left out of the fit, i.e. IRAS 08143–4406, IRAS 08281–4850, IRAS 14325–6428 and IRAS 22223+4327 respectively. The stellar temperature estimated by De Smedt et al. (2016) for IRAS 08281–4850, IRAS 14325–6428 and IRAS 22223+4327 are 7875 K, 8000 K and 6500 K and Reyniers et al. (2004) for IRAS 08143–4406 is 7150 K, while the fit of eq. (1) leads to values of 7674 K, 7211 K, 6809 K and 6856 K respectively.

In late-PAGB stars ($4500 \leq T_{\text{eff}} \leq 5500 \text{ K}$), on the other hand, is possible to determine the effective temperature from the G-band at $\lambda 4302 \text{ \AA}$. In spite of only 5 stars are present in the fit, is possible therefore to determine the effective temperature applying a linear fit

$$T_{\text{eff}} = (6291 \pm 246) - (417 \pm 81)(\text{Gband}). \quad (2)$$

The equation (2) is valid for a range in the equivalent widths between $1.76 \leq T_{\text{eff}} \leq 4.08 \text{ \AA}$ and where the standard deviation reached is $\pm 207 \text{ K}$. Two objects are left out of this relationship, IRAS 01259+6823 (5000 K), IRAS 22223+4327 (4500 K) and the fit for both objects reaches the same temperature value of 4788 K.

The stellar temperature for identified cold PAGB stars can be increased by using the resonance Ca I ($\lambda 4226 \text{ \AA}$) line. This line is sensitive to temperature, since it grows gradually from the G-type to the early K-type stars being stronger in those stars with mid-K. A lineal relationship can be obtained by adjusting the temperature and the Ca I equivalent widths for four calibrating stars, this is

$$T_{\text{eff}} = (5381 \pm 118) - (436 \pm 76)(\text{Ca I}), \quad (3)$$

where its standard deviation reaches a value of $\pm 175 \text{ K}$ and the validation range for equivalent widths can be found between 0.40 \AA and 2.31 \AA and the temperature between $\lambda 4550 \text{ \AA}$ and $\lambda 5200 \text{ \AA}$. The

results of effective temperature estimated by equations (1), (2) and (3) are in the third and fourth column of Tables 4 and 5. In the top of Figure 4, we note the dependence of the Ca I K-line and the G-band with the effective temperature (see left and right panels).

3.2. Log g's calibration

In warm stars, we can estimate the surface gravity using the Fe, Ti II blend at $\lambda 4172\text{-}9 \text{ \AA}$. This blend is constituted mainly by ionized lines of Fe and Ti and has been considered as indicator as luminosity in A-F type stars. A lineal fit leads to the following relationship

$$\log g = (1.40 \pm 0.14) - (0.16 \pm 0.07)(\text{FeTi II}). \quad (4)$$

The range of validation of this calibration in surface gravity covers $0.50 \leq \log g \leq 1.40$, while the equivalent widths of the ionized line vary between $0.50 \leq \text{FeTi II} \leq 3.90 \text{ \AA}$. The standard deviation leads to a value of $\sigma = \pm 0.21$. Two stars fall out of the fit of eq (4), i.e. IRAS 07134+1005 and IRAS 18025–3906. According to spectral types (or effective temperature), IRAS 07134+1005 and IRAS 18025–3906 it would be expected that their equivalent widths were slightly greater than 4 \AA .

We can extend the range in the surface gravity at higher values using the O I triplet lines. Due to the limitations of the spectral range to the near infrared region, the number of O I triplet lines are very scarce. Even though their values are not report in Table 4, and we will only show the functional relationship

$$\log g = (2.20 \pm 0.20) - (0.58 \pm 0.13)(\text{OIT}), \quad (5)$$

where the range on gravity vary from 1.00 to 2.20 and their equivalent widths between 0.07 to 1.95 \AA respectively. The standard deviation leads a value of $\sigma = \pm 0.35$.

In cold stars, the surface gravity is estimated using the Sr II-line. This line has been considered as the principal luminosity discriminator for cool stars in MK classification. Unfortunately the functional relationship is built with only 3 stars and this has the following form

$$\log g = (0.74 \pm 0.23) + (0.24 \pm 0.11)(\text{Sr II}). \quad (6)$$

The range of validation of this calibration in surface gravity covers $1.00 \leq \log g \leq 1.50$, while the equivalent widths of the ionized line vary between $0.77 \leq \text{Sr II} \leq 2.95 \text{ \AA}$. The standard deviation leads to a value of $\sigma = \pm 0.20$. We can also estimate the gravity for additional cold PAGB stars 13203–5917,

16494–3930, 17317–2743 and 17388–2203 when recovering the equivalent widths of the Sr II line from the Mg II line. An error of ± 0.25 is introduced when making this estimation.

The results of surface gravity estimated by equations (4) and (6) are in the fifth and sixth column of Tables 4 and 5. In the middle of Figure 4, we see the dependence of the Fe,Ti II blend and the Sr II with regard to surface gravity (see left and right panels).

3.3. $[\text{Fe}/\text{H}]$'s calibration

For the calibration of metallicity we used only neutral Fe lines. In warm stars, we use the sum of Fe I ($\lambda 4271 \text{ \AA} + \lambda 4383 \text{ \AA}$). The best fitting that recovers the metallicity is generated by a polinomial that have the form

$$[\text{Fe}/\text{H}] = -(0.73 \pm 0.10) + (0.14 \pm 0.05)(\text{FeIblend} + \text{FeI}). \quad (7)$$

The range of validation of this calibration on metallicity covers $-0.09 \leq [\text{Fe}/\text{H}] \leq -1.00$ dex, while the equivalent widths of Fe lines vary between $0.34 \leq \text{Fe I} \leq 4.40 \text{ \AA}$. The standard desviation for this relationship is ± 0.19 dex. Two outliers are present in this fitting; IRAS 19386 + 0155 to very low metallicity (-1.00 dex) and IRAS 20572 + 4919 to solar metallicity (-0.01 dex) respectively.

In cold stars, we employ the Fe I lines at $\lambda 4063 \text{ \AA}$ and $\lambda 4383 \text{ \AA}$. Of the 17 cold-PAGB stars only 5 objects have identified stellar parameters. For the Fe I ($\lambda 4353 \text{ \AA}$) line the five objects are available for the calibration. The best fitting that recovers the metallicity within a range of $-0.09 \leq [\text{Fe}/\text{H}] \leq -0.80$ dex, involves a lineal polynomial for Fe I line at $\lambda 4383 \text{ \AA}$, that is

$$[\text{Fe}/\text{H}] = -(0.92 \pm 0.16) + (0.38 \pm 0.13)(\text{FeI}), \quad (8)$$

where the range of equivalent widths vary between 0.48 to 1.94 \AA and the standard desviation leads a value of $\sigma = \pm 0.30$ dex.

On the contrary, the best fitting for Fe I line at $\lambda 4063 \text{ \AA}$ has the form

$$[\text{Fe}/\text{H}] = -(0.85 \pm 0.18) + (0.26 \pm 0.11)(\text{FeI}). \quad (9)$$

The range of equivalent widths vary between 0.48 to 2.86 \AA and the standard desviation leads a value of $\sigma = \pm 0.30$ dex.

The results of metallicity estimated by equations (7) and (8) are in the sixth and seventh column of Tables 4 and 5. In the bottom of Figure 4 we observe the dependence of the Fe I lines with regard to metallicity (see left and right panels).

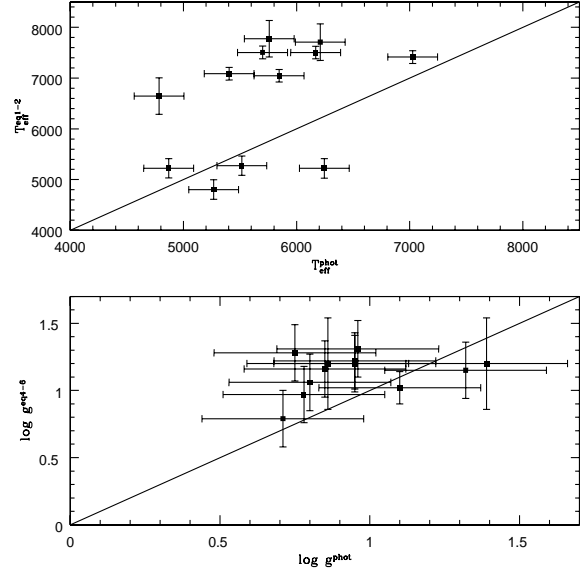


Fig. 5. Comparison between effective temperature and surface gravity obtained from 2MASS photometry by Molina (2012) and effective temperature and surface gravity estimated in this work (see upper and bottom panels). The solid stright line in each panel denotes perfect agreement between the sets of data.

4. RESULTS AND DISCUSSION

The results of the stellar parameters (columns 3, 5 and 6) for the sample studied are shown in Tables 4, 5 respectively. In general, the limitation in the spectral range and the low number of objects with identified stellar parameters lead to the fact that spectroscopic calibrations can not be applied individually to the total sample studied.

For the warm-PAGB stars, we observe that the Ca IIK line show a strong dependence on the effective temperature (see Fig. 4). However, the equivalent widths have been measured only for 9 objects out of a total of 29 identified. In order to expand the number of objects with the new values of T_{eff} , we estimate the equivalent widths of the Ca IIK line from Fe,Ti II ($\lambda 4172\text{-}9 \text{ \AA}$) blend and Fe I ($\lambda 4383 \text{ \AA}$).

Clearly this procedure introduces an uncertainty of $\pm 220 \text{ K}$ to the temperature of the additional PAGB stars, i.e. 07253–2001, 08213–3857, 11201–6545, 11387–6113, 14482–5725, 14488–5405, 15310–6149, 17208–3859, 17310–3432, 17579–3121 and 19207+2023 respectively. A similar procedure has been applied to surface gravity and metallicity in order to add new values for those objects not studied.

For surface gravity the equivalent widths of the Fe,Ti II ($\lambda 4172\text{-}9 \text{ \AA}$) blend is derived from the Mg II ($\lambda 4481 \text{ \AA}$) line and 4 PAGB stars (07253–2001,

11201–6545, 14482–5725 and 14488–5405) were added with an uncertainty of ± 0.30 . The O I ($\lambda 7771-5 \text{ \AA}$) triplet line can also be used to determine the surface gravity of those stars with $1.0 \leq \log g \leq 2.2$ respectively. According to MK classification system the O I triplet is sensitive to luminosity (or gravity).

In metallicity the neutral iron blend of Fe I ($\lambda 4271 \text{ \AA}$) is determined from Fe I ($\lambda 4383 \text{ \AA}$) line. An uncertainty of ± 0.31 dex is estimated for additional PAGB stars; 07253–2001, 08005–2356, 11201–6545, 14482–5725, 14488–5405 and 15310–6149 respectively.

In cold-PAGB stars, however, the G-band and the Fe I (4383 \AA) line have measures of equivalent widths for most objects, except the Sr II (4077 \AA) and Ca I ($\lambda 4226 \text{ \AA}$) line that is present only for 12 and 17 objects. Unfortunately, the number of objects with identified stellar parameters is very scarce, which means that the calibrations made are few unreliable. The results in the metallicity that have a subindex “a” represent the values obtained from eq. 9.

We can compare our results in T_{eff} and $\log g$ with a source whose values come from photometric calibrations for PAGB and RV Tauri stars (Molina 2012). The values of T_{eff} and $\log g$ determined from the photometric calibrations are found in the second and fourth columns of Tables 4 and 5, respectively. In the upper and bottom panels of Figure 5 we can see the comparison between the spectroscopic and photometric calibrations.

From the Figure 5 we can observe that the $T_{\text{eff}}^{\text{spec}}$ and $\log g^{\text{spec}}$ obtained spectroscopically from eq. (1) and (3) (warm stars) and from eq (2) and (5) (cold stars) are slightly higher than $T_{\text{eff}}^{\text{phot}}$ and $\log g^{\text{phot}}$ obtained photometrically from Molina’s calibrations. PAGB stars with temperature close to 5000 K seem to be adjusted satisfactorily but at a higher temperature the dispersion increase. In surface gravity, on the other hand, the spectroscopic values seem to show agreement within their uncertainties with photometric values. These results indicate that the interstellar and circumstellar reddening significantly affects the fundamental parameters when using photometric techniques.

Finally, the equivalent widths of O I T line do not show dependence to distances derived by Vickers et al.(2015).

5. SUMMARY AND CONCLUSIONS

We presented a set of spectroscopic calibrations to obtain T_{eff} , $\log g$, and $[\text{Fe}/\text{H}]$ from equivalent widths of stellar spectra. The criteria chosen for

selection of the absorption features are similar to employed by MK classification system. The equivalent widths for a total of 9 absorption features were measured.

We selected a total of 67 PAGB stars that include spectral types A and K, of which, 48 of them have a temperature between 6000 and 8000 K (warm stars) and 19 have temperature from 4500 to 5500 K (cold stars). For the determination of the spectroscopic calibrations we have identified the stellar parameters in the literature of 21 warm-PAGB stars and 5 cold-PAGB stars respectively.

We show the dependence of the stellar parameters with respect to the equivalent widths, although the limitations present in the spectral ranges make it difficult to determine the temperature, gravity and metallicity for all sample without previous studies, i.e. 27 warm-and 14 cold-PAGB stars. These calibrations would be very useful to develop suitable criteria for the rapid and accurate determination of fundamental parameters for PAGB stars. The use of only spectral criteria is very important because it allows to define the parameters for such objects, while the photometric indexes are often distorted by poor known interstellar and circumstellar reddening.

As future work it is possible to expand the spectral ranges and criteria in order to involve a great number of absorption features and to improve our spectroscopic calibrations for warm-and cold-PAGB stars using high-resolution spectra.

Acknowledgments

We are grateful to Dr. Arturo Manchado for providing us the sample of low-resolution stellar spectral. We are thankful to Carolina Foundation for financial supporting to visit to Canarias Astrophysical Institute to Spain. We thank to Dr Sunetra Giridhar, Dr Armando Arellano Ferro and Dr Valentina Klochkova for numerous comments and valuable suggestions on the text. We express our gratitude to the anonymous referee for detailed comments that have improved the interpretation of the data and text.

REFERENCES

- Alonso A., Arriba S. Martínez-Roger C., 1999, A&AS, 139, 335
- Allende-Prieto C., Majewski S.R., Schiavon R., et al., 2008, AN, 329, 1018
- Arellano Ferro, A., 2010, RMxA&A, 46, 331
- Arellano Ferro, A., Giridhar, S., Rojo Arellano, E., 2003, RMxA&A, 39, 3
- Arellano Ferro, A., Mendoza V., Eugenio E., 1993, AJ, 106, 2516
- Árnadóttir A.S., Feltzing S., Lundström I., 2010, A&A, 521, 40

- Bellinger E.P., Angelon G.C., Hekker S., Basu S., et al., 2016, *ApJ*, 830, 31
- Blanco-Cuaresma S., Soubiran C., Heiter U., Jofré P., 2014, *A&A*, 569, 111
- Castelli F., Kurucz R.L. 2003, Modelling of Stellar Atmospheres, Poster Contributions. Proceedings of the 210th Symposium of the International Astronomical Union held at Uppsala University, Uppsala, Sweden, 17-21 June, 2002. Edited by N. Piskunov, W.W. Weiss, and D.F. Gray. Published on behalf of the IAU by the Astronomical Society of the Pacific, 2003., p.A20
- Chen Y.Q., Zhao G.L., Chao R.J., Jia Y.P., Zhao J.K., et al., 2015, *RAA*, 15, 1125
- Dafonte C., Fustes D., Manteiga M., Garabato D. et al., 2016, *A&A*, 594, 68
- Damiani C., Meunier J.C., Moutou C. Delenil M. et al., 2016, *A&A*, 595, 95
- De Smedt K., van Winckel H., Kamath D., Siess L., Goriely S., Karakas A.I., Manick R., 2016, *A&A*, 587, 6
- Decin L., van Winckel H., Waelkens Ch., Bakker E.J., 1998, *A&A*, 332, 928
- Drake N.A., De la Reza R., Da Silva L., Lambert D.L., 2002, *AJ*, 123, 2703
- Fujii T., Nakada Y., Parthasarathy M., 2001, in Szczerba R., Gómy S.K., eds. *Astrophysics and Space Science Library* Vol. 265, Post-AGB objects as a Phase of Stellar Evolution. Kluwer, Dordrecht, p. 45
- García-Lario P., Manchado A., Pych W., Pottasch S.R., 1997, *A&AS*, 126, 479
- Giridhar S., Goswami A., 2002, *Bull. Astr. Soc. India*, 30, 501
- Graff P., Feroz F., Hobson M.P., Lasenby A.N., 2013, *AAS*, 22143101G
- Gray R.O., Corbally C.J., et al., *Stellar Spectral Classification*, Princeton University Press, 2009
- Gray R.O., Napier M.G., Winkler L.I., 2001, *AJ*, 121, 2148
- Gustafsson B., Edvardsson B., Eriksson K., Jorgensen U.G., Nordlund A., Plez B., 2008, *A&A*, 486, 951
- Hrivnak B.J. & Biegging J.H., 2005, *ApJ*, 624, 331
- Hrivnak B.J., Lu W., Nault K.A., 2015, *AJ*, 149, 184
- Hrivnak B.J., Kwok S., Volk K.M., 1989, *ApJ*, 346, 265
- Hu J.Y., Slijkhuis S., De Jong T. & Jiang B.W., 1993, *A&AS*, 100, 413
- Kipper T., 2008, *Baltic Astronomy*, 17, 87
- Kelly D.M. & Hrivnak B.J., 2005, *ApJ*, 629, 1040
- Klochkova V.G., 1997, *Bull. Special Astrophys. Obs.*, 44, 5
- Klochkova V.G., 2014, *Astrophys. Bull.*, 69, 279
- Klochkova V.G., Chentsov E.L., Panchuk V.E., 2008, *Astrophys. Bull.*, 63, 112
- Kovtyukh V.V., Soubiran C., Belik S.I., Gorlova N.I., 2003, *A&A*, 411, 559
- Luck R.E., 2014, *AJ*, 147, 137
- Maas T., Van Winckel H., Lloyd Evans T., 2005, *A&A*, 429, 297
- Magrini L., Randich S., Friel E., Spina L., et al., 2013, *A&A*, 558, 28
- Mauro F., Moni Bidin C., Chené A.N., Geisler D., Alonso-García J., Borissova J., Carraro G., 2013, *RMxAA&A*, 49, 189
- Min M., Jeffers S.V., Canovas H., Rodenhuis M., Keller C.U., Waters L.B.F.M., 2013, *A&A*, 554, A15
- Molina R.E., 2012, *RMxAA&A*, 48, 95
- Molina, R. & Stock, J., 2004, *RMxAA&A*, 40, 181
- Mucciarelli A., Salaris M., Lanzoni B., Pallanca C., D'lessandro E., Ferraro F.R., 2013, *ApJ*, 772, 27
- Omont A., Loup C., Forveille T., te Lintel Hekkert P., Habing H., Sivagnanam P., 1993, *A&A*, 267, 515
- Pereira C.B., Gallino R. & Bisterzo S., 2012, *A&A*, 538, 48
- Pereira C.B., Lorentz-Martins S., Machado M., 2004, *A&A*, 422, 637
- Pereira C.B., Roig F., 2006, *A&A*, 452, 571
- Ren A., Fu J., De Cat P., Wu Y. et al., 2016, *ApJS*, 225, 28
- Reyniers M. Van de Steene G.C., Van Hoof P.A.M., Van Winckel H., 2007, *A&A*, 471, 247
- Reyniers M. & Van Winckel H., 2000, *LIACO*, 35, 73
- Reyniers M., Van Winckel H., Gallino R., Straniero O., 2004, *A&A*, 417, 269
- Rose J.A., 1984, *AJ*, 89, 1238
- Sánchez-Contreras C., Sahai R., Gil de Paz A., Goodrich R., *ApJS*, 179, 166
- Schuster W.J., Nissen P.E., Parrao L., Beers T.C., Overgaard L.P., 1996, *A&AS*, 117, 317
- Soubiran C., Le Campion J.F., Cayrel de Strobel G., Caillio A., 2010, *A&A*, 515, 111
- Sousa S.G., 2014, *ARES+MOOG: A practical overview of an Equivalent Width (EW) Method to derive Stellar Parameters*, *dapb.book*, pp. 297-310
- Stephenson C.B. & Sanduleak N., 1971, *Publ. Warner & Swasey Obs.* 1, part No 1,1
- Stock, J. & Stock, J.M., 1999, *RMxAA&A*, 35, 143
- Suárez O., García-Lario P., Manchado A., Manteiga M., Ulla A., Pottasch S.R., 2006, *A&A*, 458, 173
- Sumangala Rao S., Giridhar S., Lambert D.L., 2012, *MNRAS*, 419, 1254
- Teixeira G.D.C., Sousa S.G., Tsantaki M., Monteiro M.J.P.F.G., Santos N.C., Israelian G., 2016, *A&A*, 595, 15
- Vickers S.B., Frew D.J., Parker Q.A., Bojicic I.S., 2015, *MNRAS*, 447, 1673
- Van Winckel H., Oudmaijer R.D., Trams N.R., 1996, *A&A*, 312, 553
- Waters Ch.Z., Hollek J.K., 2013, *PASP*, 125, 1164
- Wu Y., Singh H.P., Prugniel P., Gupta R., Koleva M., 2011, *A&A*, 525, 71
- Zhao G., Zhao Y.H., Chu Y.Q., Jing Y.P., Deng L.C., 2012, *RAA*, 12, 723
- Zwitter T., Siebert A., Munari U., Freeman K.C., et al. 2008, *AJ*, 136, 421

R. E. Molina: Laboratorio de Investigación en Física Aplicada y Computacional, Universidad Nacional Experimental del Táchira, Venezuela, (rmolina@unet.edu.ve).